Macromolecules
Article
Cite This: *Macromolecules* 2019, 52, 88−95
pubs.acs.org/Macromolecules

Ion Transport in Glassy Polymerized Ionic Liquids: Unraveling the Impact of the Molecular Structure

Maximilian Heres,[†] Tyler Cosby,[†] Emmanuel Urandu Mapesa,[†] Hongjun Liu,[†] Stefan Berdzinski,[§] Veronika Strehmel,[§] Mark Dadmun,[‡] Stephen J. Paddison,[†] and Joshua Sangoro*,[†]

[†]Department of Chemical and Biomolecular Engineering and [‡]Department of Chemistry, University of Tennessee, Knoxville, Tennessee 37996, United States

[§]Department of Chemistry and Institute for Coatings and Surface Chemistry, Hochschule Niederrhein University of Applied Sciences, D-47798 Krefeld, Germany

Supporting Information

ABSTRACT: The impact of molecular structure on ion dynamics and morphology in ammonium- and imidazolium-based glassy polymerized ionic liquids (polyILs) is investigated using broadband dielectric spectroscopy (BDS), wide-angle X-ray scattering (WAXS), and classical molecular dynamics (MD) simulations. It is shown that ammonium-based polyILs exhibit higher dc ionic conductivity at their respective glass transition temperatures (T_g) compared to imidazolium systems. In addition, the length of the alkyl spacer has a more drastic impact on ionic conductivity at comparable time scales of segmental dynamics for ammonium than imidazolium polyILs. Agreement between the characteristic ion diffusion lengths estimated from the dielectric data and the ion-to-ion correlation lengths from the WAXS and all-atom MD simulations is observed. A recently proposed approach is employed to determine ionic mobility in a broad frequency range spanning 5 orders of magnitude below the T_g of polyILs studied, providing access to a regime of diffusivities that is inaccessible to many current experimental techniques. The ion mobility is found to be more sensitive to variation of the molecular structure than to the effective number density of the mobile ions. These results showcase the subtle interplay between molecular structure, morphology, and ion dynamics in polymerized ionic liquids.

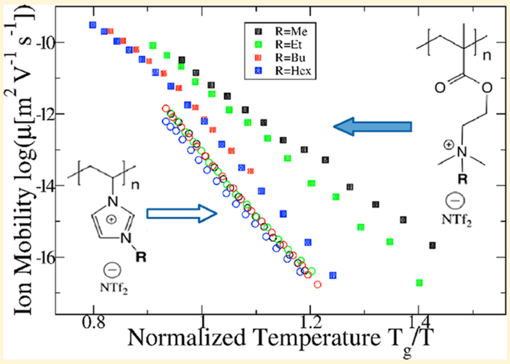

INTRODUCTION

Polymerized ionic liquids (polyILs) are a class of materials that combine the robust mechanical properties of polymers with the low flammability, low vapor pressure, and high ionic conductivity of ionic liquids (ILs).[1−10] These materials are under investigation as promising polymer electrolytes for various energy technologies such as lithium ion batteries, supercapacitors, actuators, field effect transistors, and electrochromic devices, among others.[11−16] However, the ionic conductivities of polyILs are far lower than the 10 mS/cm typically required in many practical applications. In polyILs, one type of ion is covalently attached to the side chain or backbone of the polymer chain while the counterion remains free. Recent experimental and computational studies have indicated that the untethered counterion is the dominant charge carrier in glassy polyILs.[15,17−23] It is envisaged that the key to unlocking high ionic conductivity in polyILs lies in a strategic design of chemical structures and morphologies, which permit fast, long-range counterion diffusion, while retaining the beneficial mechanical characteristics of the polymeric matrices.[24−31] However, fundamental understanding of the interplay among the chemical structure, morphology, dynamics, and ion transport in polyILs is still lacking. Furthermore, experimental techniques capable of directly probing long-range diffusion in glassy polyILs are scarce.

There are ongoing scientific efforts to understand the main parameters that control ion transport in polyILs Several ideas have been suggested for improving ion diffusion, for instance, by increasing the spacing between adjacent polymer backbones as well as tuning the cation placement position with respect to the polymer chain.[17,32−34] These studies have focused on imidazolium-based polyILs. The influence of the cation chemistry across different classes of polyILs has not been systematically investigated, especially at temperatures below the calorimetric glass transition temperatures, T_g, where the polymer segmental dynamics are slowed to the extent that ion motion is primarily dominated by the nontethered counterion. It is well established from studies of low molecular weight ionic liquids that variation of cation chemistry has a drastic impact on ionic conductivity.[35−38] It is worth noting that ion diffusion in low molecular weight ionic liquids can be measured in a fairly straightforward way using techniques such as nuclear magnetic resonance spectroscopy (NMR). However, in

Received: June 14, 2018
Revised: December 11, 2018
Published: December 18, 2018

DOI: 10.1021/acs.macromol.8b01273
Macromolecules 2019, 52, 88−95

polymerized ionic liquid systems, ion dynamics are much slower at temperatures of practical interest (around and below T_g) and cannot easily be measured by the standard NMR techniques due to low signal levels. Therefore, an open fundamental question is the role of the cation chemistry on the diffusion of ions in polyILs and how to experimentally probe ion mobilities in the glassy state.

In the current article, the impact of varying the type of polycation and the length of the alkyl functional group on ion dynamics and morphology in polyILs is investigated using BDS, wide-angle X-ray scattering (WAXS), and classical molecular dynamics (MD) simulations. Ammonium-based polyILs exhibit an emergence of long-range ordering of the polymer chains with increasing alkyl functional group length. This corresponds to a drastic decrease in ionic mobility and conductivity and an increase in the activation energy associated with ion diffusion. It is found that the T_g-independent ionic conductivity $\sigma_0(T_g/T = 1)$ of ammonium polyILs is higher by as much as 2 orders of magnitude compared to imidazolium systems. This is attributed to lower ion mobility in imidazolium polyILs due to additional restrictions of the preferred cation−anion interaction configurations. In addition, a comparison of data from the literature shows that variation of the location of the polycation relative to the polymer backbone in the vicinity of the backbone does not play a strong role for T_g-independent ionic conductivity in imidazolium polyILs even though it substantially alters their T_g.[31,32] The finding that the nature of the cation plays a more significant role in governing ion transport than the location of the cation relative to the backbone has immediate implications on the strategic design of the chemical structure of polyILs.

MATERIALS AND METHODS

Experimental Studies. The ammonium-based polymerized ionic liquids were polymerized according to a procedure reported in ref 39. Poly(1-vinyl-3-ethylimidazolium) bis(trifluoromethylsulfonyl)imide samples were polymerized according to the procedure described in Sangoro et al.[2] Glass transition temperatures and structural relaxation of the polyIL were measured using a TA Instruments Q1000 temperature-modulated differential scanning calorimeter. The calorimetric glass transition temperature conventionally corresponds to the temperature at which the structural relaxation occurs at a temperature modulation period of 100 s. The dielectric measurements were conducted using a Novocontrol High-Resolution Alpha Dielectric Analyzer (Novocontrol Technologies GmbH) over a frequency range of 10^{-1}−10^{7} Hz and a temperature range of 240−400 K, with an accuracy better than ±0.1 K. The samples were annealed in an oil-free vacuum at 30 K above their respective glass transition temperatures for 24 h. Then, the samples were pressed into 100 μm disks using a Specac Mini-Film Maker. Silica spacer rods with 100 μm diameter were included during the hot-pressing procedure to ensure uniform sample thickness during the dielectric measurements. Wide-angle X-ray scattering measurements were conducted on a SAXSLab Ganesha instrument at the Shared Materials Instrument Facility at Duke University. The samples were prepared using the same procedure as for BDS experiments and measured on the thin film stage under vacuum for 10 min at a count rate of 25 Mph/s.

Molecular Dynamics Simulations. The simulated systems of ammonium polyILs each consist of 10 40-mer polycations and 400 Tf_2N anions. All MD simulations were performed with the GROMACS package[40] using the general AMBER force field all-atom parameters following an established procedure.[40−43] A Bussi stochastic thermostat was used to control temperature,[44] while a Berendsen barostat and a Parrinello−Rahman barostat were used to control pressure.[45] NVT ensemble simulations were performed at the desired density estimated by NPT ensemble simulations at 1 atm and 400 K. The system was equilibrated for at least 50 ns, and trajectories of 50 ns were collected for structural analysis. Three independent runs were performed.

Both the direct and Fourier transform methods can be applied to calculate the structure factors of the polyILs.[18] Here, the partial structure factors are estimated by the Fourier transformation of the radial distribution function $g(r)$:

$$S_{\alpha\beta}(q) = x_\alpha\delta_{\alpha\beta} + x_\alpha x_\beta\rho_0\int_0^{L/2} 4\pi r^2[g_{\alpha\beta}(r) - 1]\frac{\sin qr}{qr}w(r)\,dr \tag{1}$$

where $\delta_{\alpha\beta}$ is the Kronecker delta, x_α is the corresponding mole fraction of α, and ρ_0 is the total number density of the system. The revised Lorch window function, $w(r) = \frac{3}{\left(\frac{2\pi r}{L}\right)^3}\left[\sin\left(\frac{2\pi r}{L}\right) - \frac{2\pi r}{L}\cos\left(\frac{2\pi r}{L}\right)\right]$, was applied to remedy the cutoff ripple artifact.[46,47] Partial structure factors were weighted with the atomic form factors leading to the total X-ray structure factor:

$$S^x(q) = \frac{1}{\sum_\alpha x_\alpha {f_\alpha}^2(q)}\sum_\alpha^n\sum_\beta^n f_\alpha(q)f_\beta(q)S_{\alpha\beta}(q) \tag{2}$$

where $f_\alpha(q)$ represents the X-ray atomic form factor of α and can be approximated with a series of Gaussian functions of q over the range of (0, 25) Å^{-1} according to

$$f_\alpha(q) = \sum_{i=1}^{4} a_i \exp\left[-b_i\left(\frac{q}{4\pi}\right)^2\right] + c \tag{3}$$

The tabulated coefficients a_i, b_i, and c are reported in Table 6.1.1.4 of the International Tables for Crystallography.[48] For neutron scattering, $f_\alpha(q)$ is replaced with the neutron scattering lengths, b_α: −3.739, 5.803, 6.646, 9.36, 5.654, 6.671, and 2.847 fm for hydrogen, oxygen, carbon, nitrogen, fluorine, deuterium, and sulfur, respectively. Hence, the total neutron structure factor is

$$S^n(q) = \frac{1}{\sum_\alpha x_\alpha {b_\alpha}^2}\sum_\alpha^n\sum_\beta^n b_\alpha b_\beta S_{\alpha\beta}(q) \tag{4}$$

RESULTS AND DISCUSSION

The long-range ion diffusion in amorphous polymerized ionic liquids below T_g, where the polymer dynamics occurs at longer time scales compared to the experimentally accessible window, can be approximated by the random barrier model (RBM). This model assumes that the motion of the charge carriers takes place through hopping in a spatially randomly varying energy landscape.[49] The dielectric spectra of poly(2-trimethylammoniumethyl) methacrylate bis(trifluoromethylsulfonyl)imide are presented in Figure 1 in terms of the real and imaginary parts of complex dielectric function, ε^*, and complex conductivity, σ^*. The spectra are well described by a combination of the RBM and Havriliak−Negami (HN) fitting functions:[50,51]

$$\sigma^*(\omega) = \frac{\sigma_0\frac{i\omega}{\omega_\sigma}}{\ln\left(1 + \frac{i\omega}{\omega_\sigma}\right)} + \frac{i\omega\varepsilon_0\Delta\varepsilon}{\left(1 + \left(\frac{i\omega}{\omega_{\mathrm{HN}}}\right)^\beta\right)^\gamma} + i\omega\varepsilon_0\varepsilon_\infty \tag{5}$$

where ω_σ, σ_0, ε_0, $\Delta\varepsilon$, ε_∞, and ω_{HN} denote the radial frequency characterizing the onset of long-range ion diffusion and the resulting frequency-independent dc ionic conductivity, the permittivity of free space, the dielectric relaxation strength, the high frequency value of the real part of the dielectric function, and the HN relaxation rate, respectively. In addition, β and γ are spectral shape parameters. A successful ion jump inevitably results in rearrangement of the microscopic environment

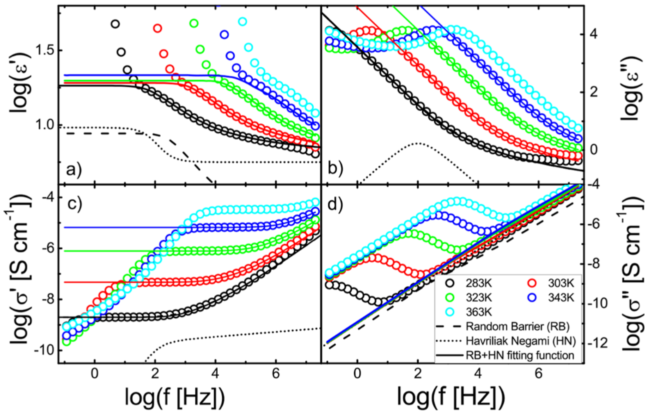

Figure 1. Real and imaginary part of the complex dielectric function, $\varepsilon^*(\omega) = \varepsilon'(\omega) - i\varepsilon''(\omega)$, and complex conductivity function, $\sigma^*(\omega) = \sigma'(\omega) + i\sigma''(\omega)$, for poly(2-trimethylammoniumethyl) methacrylate bis(trifluoromethylsulfonyl)imide. Solid lines are fits to the real and imaginary parts of complex conductivity using a combination of the analytical approximation of the RBM and two Havriliak−Negami functions. Fit parameters are tabulated in the Supporting Information. In this work, the error bars are smaller than the size of the symbols, unless otherwise indicated.

around the ion. The additional polarization arising from reorientation motion caused by the ion diffusion is accounted for by the empirical HN function. Furthermore, the faster secondary dipolar relaxations are described by an additional HN function. At sufficiently long time scales the mobile ions begin to accumulate at the electrodes leading to relaxation-like features termed electrode polarization, which has been shown to depend on several factors including sample geometry, material of electrodes, and bulk transport properties of the material under study.[52−55] Thus, detailed analysis of electrode polarization is beyond the scope of this study.

Figure 2 presents the dc ionic conductivity, σ_0, versus inverse temperature as well as the T_g-normalized temperature, as obtained from the random barrier model fits. Increasing alkyl chain length from methyl to hexyl in the polyammoniums results in the reduction ionic conductivity at T_g by 2 orders of magnitude. In contrast, the influence of alkyl chain length on σ_0 of the polyimidazolium is rather weak. The origin of the discrepancy between alkyl chain length effects in the studied imidazolium polyILs has been attributed to the influence of cation placement with respect to the backbone of the polymer chain.[3,9,32] In agreement with this picture, the cation in the vinylimidazolium is located much closer to the polymer backbone, and therefore the influence of increasing backbone-to-backbone spacing has a minimal impact on the T_g-independent ionic conductivity. However, comparing the T_g-independent ionic conductivities of imidazolium polyILs derived from acrylate and vinyl monomers as well as with the imidazolium contained in the polymer backbone itself reveals the surprising fact that the position of the imidazolium cation in the polymer has no apparent effect on the T_g-independent ionic conductivities near the glass-transition temperature, in contrast to some recent results.[31,32] In systems where the polycation is spaced sufficiently far from the polymer backbone, the flexibility of the ionic group with respect to the polymer chain might ultimately influence the T_g independent ionic conductivity, causing breakdown of the observed invariance. Comparing the ammonium- and imidazolium-based polymerized ionic liquids featuring butyl chains reveals that the former systems have higher ionic conductivities when factors such as polymer backbone, alkyl chain length, and anion are constant (Figure 3). This is in qualitative agreement with findings for ammonium- and imidazolium-based low molecular weight ionic liquids.[56] In this work, it was concluded that the σ_0 is higher for the ammonium systems due to the molecular structure of the ammonium cation, which provides a better shielding of electrostatic interactions with the anion compared to the imidazolium cation.[57]

Insight into the origin of the changes in ionic conductivity of the polyammonium cations may be obtained by analyzing the ion dynamics below T_g, where the anion motion is not aided by polymer segmental dynamics. The temperature dependence of σ_0 transitions from a Vogel−Fulcher−Tammann (VFT) to Arrhenius behavior when the material is cooled to the glassy state.[2,34,51,58] This behavior is characteristic for many ion conducting glass-formers, since ion diffusion is assisted by structural relaxations above the glass transition temperature, while ionic conductivity below the glass transition is dominated solely by the untethered counterion diffusion.[2,59−62] The activation energy governing the anion motion, E_a, below T_g, can be obtained from the temperature dependence of ionic conductivity using the Arrhenius equation $\sigma_0 = \sigma_\infty e^{-E_a/k_BT}$, where σ_∞ is a pre-exponential factor and k_B is the Boltzmann constant. The values of activation energy thus obtained are presented in the Supporting Information (Figure S1 and Table S1). E_a increases from 75 to 114 kJ mol^{-1} with increasing alkyl chain length for the ammonium-based polyILs

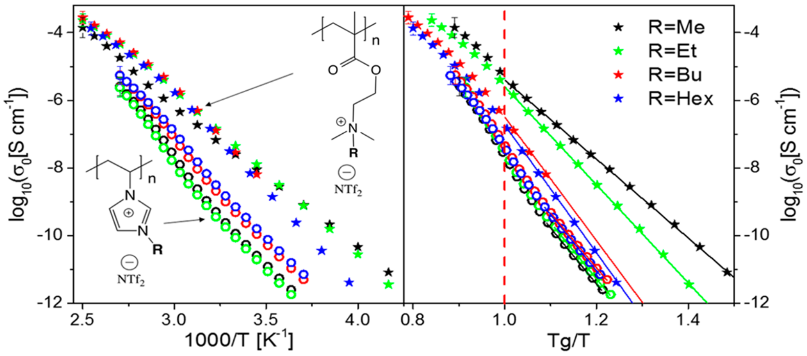

Figure 2. Plots of dc ionic conductivity versus inverse temperature and T_g-independent ionic conductivity for ammonium (stars) and imidazolium (open circles) based polymerized ionic liquids. Solid lines indicate Arrhenius fits of ionic conductivity below T_g to determine the activation energy associated with ion transport. The red dashed line indicates $T_g = T$.

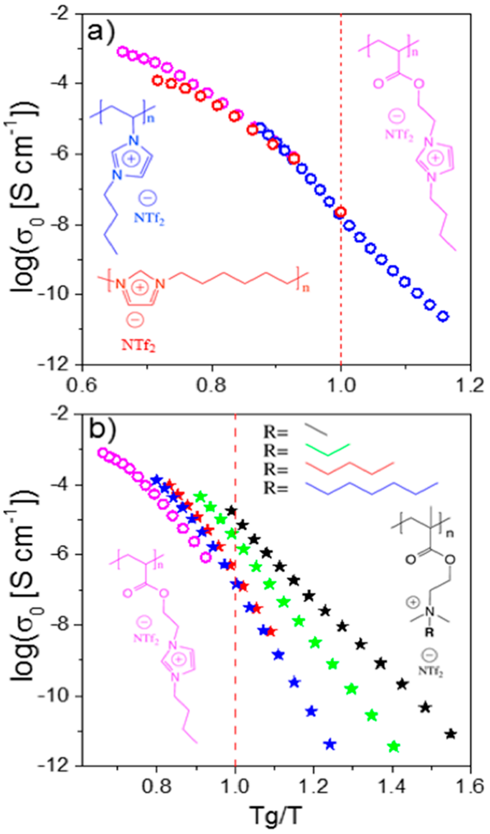

Figure 3. T_g-independent ionic conductivity for imidazolium-based polymerized ionic liquids with varying cation position (a) methacrylate side-chain polyIL with ammonium and imidazolium cation (b). The red dashed line indicates $T = T_g$. The magenta and red data are from published literature.[30,32]

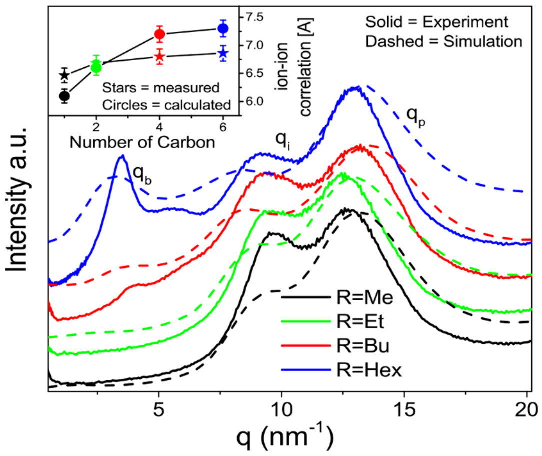

Figure 4. Experimentally determined wide-angle X-ray scattering (WAXS) data for ammonium-based polyIL with varying alkyl chain lengths, showing backbone-to-backbone correlation distances, q_b, ion-to-ion correlation distance, q_i, and pendant-to-pendant group correlation lengths, q_p are indicated by solid lines. Dashed lines show molecular dynamics simulation results of the X-ray spectra. The inset shows mean characteristic ion diffusion distances calculated from BDS data (circles) and ion-to-ion correlation distances measured by WAXS (stars) where correlation distance $d = 2\pi/q$.

but remains a constant 105 ± 2 kJ mol^{-1} for the imidazolium systems. It is worth noting that the values of E_a obtained from σ_0 and ω_σ are practically equivalent (Figure S1 and Table S1). The change in E_a for the polyammonium systems indicates a potential change in the ion transport mechanism with increasing alkyl chain length. The energy barrier determining ion diffusion in the glassy state can be approximately related to the mean diffusion distance by the equation[63,64] $E_a = \frac{\lambda^2 \upsilon_0^2 m_{\mathrm{anion}}}{2}$ where λ is the characteristic mean diffusion length, υ_0 is the attempt frequency, and m_{anion} is the molar mass of the anion. The attempt frequencies for ion conducting materials are typically around 10^{12} Hz.[65] An attempt frequency of 1.0×10^{12} Hz yields a characteristic diffusion length of 7 Å for the polyimidazoliums. This distance is in good agreement with the ion−ion correlation distance obtained via X-ray measurements and molecular dynamics simulations.[18,64] In contrast, the average distance separating anions in neighboring chains, which corresponds to the backbone-to-backbone correlation distance, ranges from 15 to 20 Å at these alkyl chain lengths. Utilizing the same attempt frequency for the ammonium systems yields a mean jump length of only 6 Å, which increases to 7.3 Å when the alkyl chain length increases to hexyl as seen in the inset in Figure 4. These values are much longer than mean ion jump lengths found for low molecular weight ILs, and the two cannot not be regarded as identical physical quantities.

To check the validity of the calculated lengths, wide-angle X-ray scattering (WAXS) measurements and corresponding atomistic molecular dynamics simulations were carried out. Figure 4 shows WAXS spectra of the ammonium-based polyIL. Based on previous data for poly(methyl methacrylate) and imidazolium-based polyILs, the peaks were found to correspond to the pendant group correlation distance, q_p, the ion-to-ion correlation lengths, q_i, and the backbone-to-backbone spacing, q_b.[17,66,67] PolyILs with butyl and hexyl pendant groups show signatures of long-range order corresponding to q_b. However, this peak is not observed in methyl and ethyl samples. This is not because there is an absence of order in the backbone packing in these short side-chain samples, but rather a result of poor contrast to observe this packing in the X-ray scattering experiments. This picture is verified by MD simulations that show the neutron scattering patterns of deuterated analogues which reveal the existence of peaks corresponding to backbone-to-backbone correlation distances in the short chain ammonium systems as well. Figure 5 displays this neutron scattering simulation data for deuterated and perdeuterated ammonium-based polyILs. In the neutron scattering simulations, a peak corresponding to the backbone-to-backbone distances is clearly visible for all samples studied. Similar simulations have been previously performed for a series of imidazolium-based samples and compared to measured neutron scattering data.[4] Simulations of the neutron scattering profiles also reveal an interesting configuration when comparing the length of the side chain of the polymer to the backbone-to-backbone distances. For methyl and ethylammonium polymerized ionic liquids, the projected side chain length is less than half the distance between neighboring backbones, indicating no interaction between side chains of neighboring polymers (inset Figure 5b). For polyILs with butyl and hexyl pendant groups, however, the projected side-chain distance exceeds half of the backbone-to-backbone distance, suggesting the formation of interpolymer interaction of side chains. We conjecture that this is due to

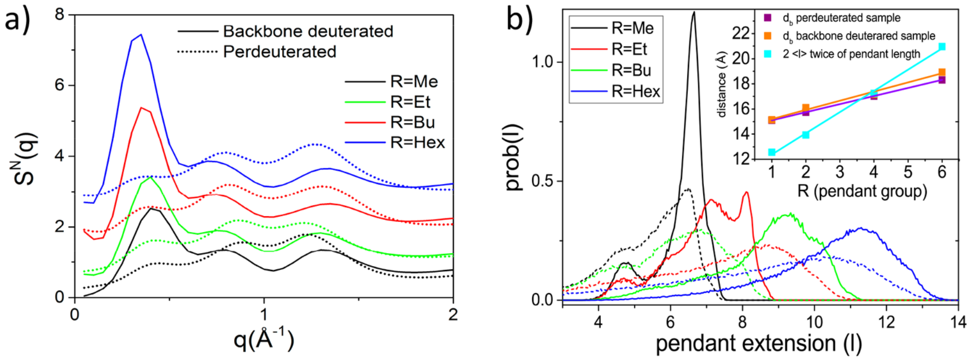

Figure 5. Neutron scattering simulation of deuterated and perdeuterated ammonium-based polymerized ionic liquids with alkyl chain length, *R*, ranging from methyl to hexyl shown in (a) for samples with deuterated backbone and perdeuterated side chains. The probability associated with the distance between backbone to the end of pendant group are shown in (b) for extended and projected distances in solid and dotted lines, respectively. The distances obtained from (a) and (b) are shown in the inset of (b) as functions of alkyl chain length for the series of polyILs.

formation of nonpolar regions resulting from aggrregation of alkyl chains of neighboring pendant groups that can hinder anion mobility.

The WAXS (see also Figure S2) and neutron scattering spectra of chain-deuterated and perdeuterated samples from the molecular dynamics simulations can reproduce the pendant group, ion-to-ion, and the backbone-to-backbone correlation distances. For methyl- and ethylammonium-based systems, the backbone-to-backbone spacing is 15 and 15.3 Å, while the projected length of the side chain is only 6.2 and 6.8 Å, respectively. This indicates minimal interaction between pendant groups of neighboring chains. However, for the pendant group length of the butyl and hexyl systems, the length of the projected side chain, 8 and 11 Å, meets or exceeds the length of half of the backbone-to-backbone spacing, which is only 16 and 17 Å, respectively. Side chains of neighboring polyILs with longer alkyl chains are therefore able to interact and form nonpolar regions between neighboring chains. This change in local ordering can hinder the path of the diffusing ions, resulting in higher activation energies associated with ion diffusion and, hence, lower ionic conductivity.

The measured ion-to-ion correlation lengths for the ammonium-based polyIL correspond well with the estimated characteristic diffusion lengths calculated from the activation energy of anion diffusion in the glassy state. To a good approximation, the characteristic diffusion length calculated from the temperature dependence of σ_0 can be assumed to correspond to the distance between minima of adjacent potential energy height that determine long-range ion motion. The energy landscape for a diffusing counterion would exhibit a minimum when counterion and polyion interact closely. Therefore, the simplistic picture correlating the characteristic diffusion length calculated from the dielectric spectra to the ion−ion correlation length measured via WAXS and obtained from molecular dynamics simulations could be valid.

A comparison of calculated mean characteristic ion diffusion distances and measured ion-to-ion correlation lengths is provided in Table S1. Interpreting ω_σ as the inverse of the characteristic residence time of the mobile ions in the bottom of the potential wells associated with the energy barriers which determine long-range diffusion, the Einstein−Smoluchowski relation can be employed to calculate the effective diffusion coefficient. Within this framework, the mean diffusion coefficient is given by $D = \lambda^2\omega\sigma/6$. In addition, the ion (charge carrier) mobility is obtained from the Einstein relation. Figure 6 shows an estimate of the charge carrier mobility, μ, which is obtained based on the mean diffusion lengths calculated from BDS data, using the relation[50] $\mu = q\lambda^2\omega\sigma/6k_BT$ where q is the elementary charge. The effective number density of charge carriers, $n = \sigma_0/q\mu$, is comparable for ammonium- and imidazolium-based polyILs in this study.[6] While anion mobility values are comparable among the polyimidazolium systems, the polyammoniums show a substantial slowing down of anion mobility with increasing alkyl chain length at the same values of T_g/T (Figure 6). The differences in the ionic conductivity between the two classes of polyILs investigated therefore stem primarily from the disparities in the ion mobility. This is consistent with previous results for ammonium- and imidazolium-based low molecular weight ionic liquids, that the σ_0 is higher for the ammonium systems due to the chemical structure of the ammonium cation, which provides a more effective shielding of the interactions with the anion compared to the imidazolium cation.[56]

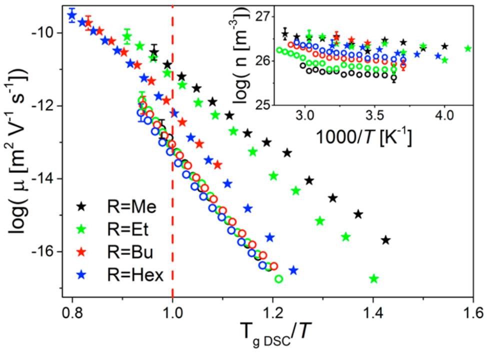

Figure 6. Ion mobilities of ammonium (stars) and imidazolium (circles) based polymerized ionic liquids as a function of T_g-normalized temperature. The red dashed line marks $T = T_g$. The inset shows the calculated number density of charge carriers.

These results suggest that the ion chemistry and morphology in polymerized ionic liquids can result in hindrance of the ion diffusion paths, for example, by allowing the formation of restrictive nonpolar regions between polymer chains, causing a decrease in the ion mobility, and with it a decrease in T_g-independent ionic conductivity. Furthermore, shorter ion-to-ion correlation lengths result in lower activation energy of ion diffusion below T_g and thus also facilitate ion conduction. The weak influence of alkyl chain length on conductivity as reported for imidazolium systems is in accord with the structural finding that ion-to-ion correlation distances in these systems are invariant with changing alkyl chain length.[17,18,64,68] In addition, the proposed approach to obtain diffusivities enables experimental determination of ion mobilities in the glassy state over a broad range spanning over 6 orders of magnitude. The absolute values of ion mobilities accessible via the proposed method are too low to be measured by any of the standard techniques such as field gradient NMR. These findings provide an important fundamental understanding of ion transport in polymerized ionic liquids and will be useful in the strategic design of materials with enhanced ionic conductivity for solid polymer electrolytic applications.

■ CONCLUSIONS

Ion transport and morphology in a series of ammonium- and imidazolium-based polymerized ionic liquids are investigated by BDS, WAXS, and MD simulations. Ammonium-based polyILs show drastic but systematic changes in their ion transport properties with increasing alkyl functional group length, a phenomenon which is practically absent in imidazolium systems. A recent approach to determine ion mobility in a broad frequency range spanning over 5 orders of magnitude below the glass transition temperatures (T_g) of polymerized ionic liquids is employed.[23] T_g-independent ionic conductivity reveals a strong correlation between alkyl spacer group length and ion dynamics in the ammonium-based polymerized ionic liquids, whereas imidazolium systems appear relatively unaffected. This work demonstrates that the ion chemistry and local morphology of the polymerized cation play a more important role than the position of the cation with respect to the polymer chain. These results showcase the subtle interplay between molecular structure, morphology, and ion dynamics in polymerized ionic liquids.

■ ASSOCIATED CONTENT

Ⓢ Supporting Information

The Supporting Information is available free of charge on the ACS Publications website at DOI: 10.1021/acs.macromol.8b01273.

Activation energies calculated from dielectric data; DSC, WAXS, and MD simulations data (PDF)

■ AUTHOR INFORMATION

Corresponding Author

*E-mail jsangoro@utk.edu; phone (865) 974-4395 (J.S.).

ORCID

Tyler Cosby: 0000-0001-6381-558X
Emmanuel Urandu Mapesa: 0000-0002-2206-0990
Hongjun Liu: 0000-0003-3326-2640
Mark Dadmun: 0000-0003-4304-6087
Stephen J. Paddison: 0000-0003-1064-8233
Joshua Sangoro: 0000-0002-5483-9528

Notes

The authors declare no competing financial interest.

■ ACKNOWLEDGMENTS

M.H., E.U.M., and J.S. gratefully acknowledge support by the National Science Foundation, Division of Materials Research, Polymers Program through DMR-1508394. T.C. gratefully acknowledges financial support from the U.S. Army Research Office under Contract W911NF-17-1-0052. H.L. and S.J.P. are grateful for financial support from the U.S. Army Research Office under Contract W911NF-15-1-0501. This work was performed in part at the Duke University Shared Materials Instrumentation Facility (SMIF), a member of the North Carolina Research Triangle Nanotechnology Network (RTNN), which is supported by the National Science Foundation (Grant ECCS-1542015) as part of the National Nanotechnology Coordinated Infrastructure (NNCI). Computing resources were provided through the XSEDE allocation DMR130078.

■ REFERENCES

(1) Armand, M.; Endres, F.; MacFarlane, D. R.; Ohno, H.; Scrosati, B. Ionic-liquid materials for the electrochemical challenges of the future. *Nat. Mater.* **2009**, *8* (8), 621−629.

(2) Sangoro, J. R.; Iacob, C.; Agapov, A. L.; Wang, Y.; Berdzinski, S.; Rexhausen, H.; Strehmel, V.; Friedrich, C.; Sokolov, A. P.; Kremer, F. Decoupling of ionic conductivity from structural dynamics in polymerized ionic liquids. *Soft Matter* **2014**, *10* (20), 3536−3540.

(3) Yuan, J.; Mecerreyes, D.; Antonietti, M. Poly(ionic liquid)s: An update. *Prog. Polym. Sci.* **2013**, *38* (7), 1009−1036.

(4) Ohno, H.; Yoshizawa, M.; Ogihara, W. Development of new class of ion conductive polymers based on ionic liquids. *Electrochim. Acta* **2004**, *50* (2−3), 255−261.

(5) Sangoro, J.; Iacob, C.; Serghei, A.; Naumov, S.; Galvosas, P.; Kärger, J.; Wespe, C.; Bordusa, F.; Stoppa, A.; Hunger, J.; Buchner, R.; Kremer, F. Electrical conductivity and translational diffusion in the 1-butyl-3-methylimidazolium tetrafluoroborate ionic liquid. *J. Chem. Phys.* **2008**, *128* (21), 214509.

(6) Sangoro, J. R.; Kremer, F. Charge Transport and Glassy Dynamics in Ionic Liquids. *Acc. Chem. Res.* **2012**, *45* (4), 525−532.

(7) Ueki, T.; Watanabe, M. Macromolecules in Ionic Liquids: Progress, Challenges, and Opportunities. *Macromolecules* **2008**, *41* (11), 3739−3749.

(8) Yin, K.; Zhang, Z.; Yang, L.; Hirano, S.-I. An imidazolium-based polymerized ionic liquid via novel synthetic strategy as polymer electrolytes for lithium ion batteries. *J. Power Sources* **2014**, *258*, 150−154.

(9) Yuan, J.; Antonietti, M. Poly(ionic liquid)s: Polymers expanding classical property profiles. *Polymer* **2011**, *52* (7), 1469−1482.

(10) Jo, G.; Ahn, H.; Park, M. J. Simple Route for Tuning the Morphology and Conductivity of Polymer Electrolytes: One End Functional Group is Enough. *ACS Macro Lett.* **2013**, *2* (11), 990−995.

(11) Chen, X.; Zhao, J.; Zhang, J.; Qiu, L.; Xu, D.; Zhang, H.; Han, X.; Sun, B.; Fu, G.; Zhang, Y.; Yan, F. Bis-imidazolium based poly(ionic liquid) electrolytes for quasi-solid-state dye-sensitized solar cells. *J. Mater. Chem.* **2012**, *22* (34), 18018−18024.

(12) Wang, Y.; Chen, K. S.; Mishler, J.; Cho, S. C.; Adroher, X. C. A review of polymer electrolyte membrane fuel cells: Technology, applications, and needs on fundamental research. *Appl. Energy* **2011**, *88* (4), 981−1007.

(13) Mecerreyes, D. Polymeric ionic liquids: Broadening the properties and applications of polyelectrolytes. *Prog. Polym. Sci.* **2011**, *36* (12), 1629−1648.

(14) Lin, B.; Qiu, L.; Lu, J.; Yan, F. Cross-Linked Alkaline Ionic Liquid-Based Polymer Electrolytes for Alkaline Fuel Cell Applications. *Chem. Mater.* **2010**, *22* (24), 6718−6725.

(15) Heres, M.; Cosby, T.; Mapesa, E. U.; Sangoro, J. Probing Nanoscale Ion Dynamics in Ultrathin Films of Polymerized Ionic Liquids by Broadband Dielectric Spectroscopy. *ACS Macro Lett.* **2016**, *5* (9), 1065−1069.

(16) Bandomir, J.; Schulz, A.; Taguchi, S.; Schmitt, L.; Ohno, H.; Sternberg, K.; Schmitz, K.-P.; Kragl, U. Synthesis and Character-

ization of Polymerized Ionic Liquids: Mechanical and Thermal Properties of a Novel Type of Hydrogels. *Macromol. Chem. Phys.* **2014**, *215* (8), 716−724.

(17) Iacob, C.; Matsumoto, A.; Brennan, M.; Liu, H.; Paddison, S. J.; Urakawa, O.; Inoue, T.; Sangoro, J.; Runt, J. Polymerized Ionic Liquids: Correlation of Ionic Conductivity with Nanoscale Morphology and Counterion Volume. *ACS Macro Lett.* **2017**, *6* (9), 941−946.

(18) Liu, H.; Paddison, S. J. Direct Comparison of Atomistic Molecular Dynamics Simulations and X-ray Scattering of Polymerized Ionic Liquids. *ACS Macro Lett.* **2016**, *5* (4), 537−543.

(19) Nakamura, K.; Fukao, K.; Inoue, T. Dielectric Relaxation and Viscoelastic Behavior of Polymerized Ionic Liquids with Various Counteranions. *Macromolecules* **2012**, *45* (9), 3850−3858.

(20) Nakamura, K.; Saiwaki, T.; Fukao, K. Dielectric Relaxation Behavior of Polymerized Ionic Liquid. *Macromolecules* **2010**, *43* (14), 6092−6098.

(21) Marcilla, R.; Alcaide, F.; Sardon, H.; Pomposo, J. A.; Pozo-Gonzalo, C.; Mecerreyes, D. Tailor-made polymer electrolytes based upon ionic liquids and their application in all-plastic electrochromic devices. *Electrochem. Commun.* **2006**, *8* (3), 482−488.

(22) Nakamura, K.; Fukao, K. Dielectric relaxation behavior of polymerized ionic liquids with various charge densities. *Polymer* **2013**, *54* (13), 3306−3313.

(23) Harris, M. A.; Heres, M. F.; Coote, J.; Wenda, A.; Strehmel, V.; Stein, G. E.; Sangoro, J. Ion Transport and Interfacial Dynamics in Disordered Block Copolymers of Ammonium-Based Polymerized Ionic Liquids. *Macromolecules* **2018**, *51* (9), 3477−3486.

(24) Chen, H.; Choi, J.-H.; Salas-de la Cruz, D.; Winey, K. I.; Elabd, Y. A. Polymerized Ionic Liquids: The Effect of Random Copolymer Composition on Ion Conduction. *Macromolecules* **2009**, *42* (13), 4809−4816.

(25) Matsumi, N.; Sugai, K.; Miyake, M.; Ohno, H. Polymerized Ionic Liquids via Hydroboration Polymerization as Single Ion Conductive Polymer Electrolytes. *Macromolecules* **2006**, *39* (20), 6924−6927.

(26) Mogurampelly, S.; Keith, J. R.; Ganesan, V. Mechanisms Underlying Ion Transport in Polymerized Ionic Liquids. *J. Am. Chem. Soc.* **2017**, *139* (28), 9511−9514.

(27) Gainaru, C.; Stacy, E. W.; Bocharova, V.; Gobet, M.; Holt, A. P.; Saito, T.; Greenbaum, S.; Sokolov, A. P. Mechanism of Conductivity Relaxation in Liquid and Polymeric Electrolytes: Direct Link between Conductivity and Diffusivity. *J. Phys. Chem. B* **2016**, *120* (42), 11074−11083.

(28) Nishimura, N.; Ohno, H. 15th anniversary of polymerised ionic liquids. *Polymer* **2014**, *55* (16), 3289−3297.

(29) Nakamura, K.; Saiwaki, T.; Fukao, K.; Inoue, T. Viscoelastic Behavior of the Polymerized Ionic Liquid Poly(1-ethyl-3-vinylimidazolium bis(trifluoromethanesulfonylimide)). *Macromolecules* **2011**, *44* (19), 7719−7726.

(30) Ye, Y.; Choi, J.-H.; Winey, K. I.; Elabd, Y. A. Polymerized Ionic Liquid Block and Random Copolymers: Effect of Weak Microphase Separation on Ion Transport. *Macromolecules* **2012**, *45* (17), 7027−7035.

(31) Ye, Y.; Elabd, Y. A. Anion exchanged polymerized ionic liquids: High free volume single ion conductors. *Polymer* **2011**, *52* (5), 1309−1317.

(32) Evans, C. M.; Bridges, C. R.; Sanoja, G. E.; Bartels, J.; Segalman, R. A. Role of Tethered Ion Placement on Polymerized Ionic Liquid Structure and Conductivity: Pendant versus Backbone Charge Placement. *ACS Macro Lett.* **2016**, *5* (8), 925−930.

(33) Fan, F.; Wang, W.; Holt, A. P.; Feng, H.; Uhrig, D.; Lu, X.; Hong, T.; Wang, Y.; Kang, N.-G.; Mays, J.; Sokolov, A. P. Effect of Molecular Weight on the Ion Transport Mechanism in Polymerized Ionic Liquids. *Macromolecules* **2016**, *49* (12), 4557−4570.

(34) Fan, F.; Wang, Y.; Hong, T.; Heres, M. F.; Saito, T.; Sokolov, A. P. Ion Conduction in Polymerized Ionic Liquids with Different Pendant Groups. *Macromolecules* **2015**, *48* (13), 4461−4470.

(35) Dong, K.; Liu, X.; Dong, H.; Zhang, X.; Zhang, S. Multiscale Studies on Ionic Liquids. *Chem. Rev.* **2017**, *117* (10), 6636−6695.

(36) Griffin, P. J.; Freyer, J. L.; Han, N.; Geller, N.; Yin, X.; Gheewala, C. D.; Lambert, T. H.; Campos, L. M.; Winey, K. I. Ion Transport in Cyclopropenium-Based Polymerized Ionic Liquids. *Macromolecules* **2018**, *51* (5), 1681−1687.

(37) Griffin, P. J.; Holt, A. P.; Tsunashima, K.; Sangoro, J. R.; Kremer, F.; Sokolov, A. P. Ion transport and structural dynamics in homologous ammonium and phosphonium-based room temperature ionic liquids. *J. Chem. Phys.* **2015**, *142* (8), 084501.

(38) Cosby, T.; Holt, A.; Griffin, P. J.; Wang, Y.; Sangoro, J. Proton Transport in Imidazoles: Unraveling the Role of Supramolecular Structure. *J. Phys. Chem. Lett.* **2015**, *6* (19), 3961−3965.

(39) Strehmel, V.; Berdzinski, S.; Ehrentraut, L.; Faßbender, C.; Horst, J.; Leeb, E.; Liepert, J.; Ruby, M. P.; Senkowski, V.; Straßburg, P.; Wenda, A.; Strehmel, C. Application of ionic liquids in synthesis of polymeric binders for coatings. *Prog. Org. Coat.* **2015**, *89*, 297−313.

(40) Hess, B.; Kutzner, C.; van der Spoel, D.; Lindahl, E. GROMACS 4: Algorithms for Highly Efficient, Load-Balanced, and Scalable Molecular Simulation. *J. Chem. Theory Comput.* **2008**, *4* (3), 435−447.

(41) Liu, H.; Maginn, E. A molecular dynamics investigation of the structural and dynamic properties of the ionic liquid 1-n-butyl-3-methylimidazolium bis(trifluoromethanesulfonyl)imide. *J. Chem. Phys.* **2011**, *135* (12), 124507.

(42) Liu, H.; Paddison, S. J. Direct calculation of the X-ray structure factor of ionic liquids. *Phys. Chem. Chem. Phys.* **2016**, *18* (16), 11000−11007.

(43) Liu, H.; Paddison, S. J. Alkyl Chain Length Dependence of Backbone-to-Backbone Distance in Polymerized Ionic Liquids: An Atomistic Simulation Perspective on Scattering. *Macromolecules* **2017**, *50* (7), 2889−2895.

(44) Bussi, G.; Donadio, D.; Parrinello, M. Canonical sampling through velocity rescaling. *J. Chem. Phys.* **2007**, *126* (1), 014101.

(45) Parrinello, M.; Rahman, A. Crystal Structure and Pair Potentials: A Molecular-Dynamics Study. *Phys. Rev. Lett.* **1980**, *45* (14), 1196−1199.

(46) Soper, A. K.; Barney, E. R. On the use of modification functions when Fourier transforming total scattering data. *J. Appl. Crystallogr.* **2012**, *45* (6), 1314−1317.

(47) Lorch, E. Neutron diffraction by germania, silica and radiation-damaged silica glasses. *J. Phys. C: Solid State Phys.* **1969**, *2* (2), 229.

(48) Brown, P. J.; Fox, A. G.; Maslen, E. N.; O'Keefe, M. A.; Willis, B. T. M. Intensity of diffracted intensities. In *International Tables for Crystallography*; John Wiley & Sons, Ltd.: 2006.

(49) Dyre, J. C. The random free-energy barrier model for ac conduction in disordered solids. *J. Appl. Phys.* **1988**, *64* (5), 2456−2468.

(50) Kremer, F.; Schönhals, A. *Broadband Dielectric Spectroscopy*; Springer-Verlag: Berlin, 2003.

(51) Dyre, J. C.; Christensen, T.; Olsen, N. B. Elastic models for the non-Arrhenius viscosity of glass-forming liquids. *J. Non-Cryst. Solids* **2006**, *352* (42−49), 4635−4642.

(52) Wang, Y.; Sun, C. N.; Fan, F.; Sangoro, J. R.; Berman, M. B.; Greenbaum, S. G.; Zawodzinski, T. A.; Sokolov, A. P. Examination of methods to determine free-ion diffusivity and number density from analysis of electrode polarization. *Physical review. E, Statistical, nonlinear, and soft matter physics* **2013**, *87* (4), 042308.

(53) Serghei, A.; Tress, M.; Sangoro, J. R.; Kremer, F. Electrode polarization and charge transport at solid interfaces. *Phys. Rev. B: Condens. Matter Mater. Phys.* **2009**, *80* (18), 184301/1−184301/5.

(54) Sangoro, J. R.; Serghei, A.; Naumov, S.; Galvosas, P.; Karger, J.; Wespe, C.; Bordusa, F.; Kremer, F. Charge transport and mass transport in imidazolium-based ionic liquids. *Physical review. E, Statistical, nonlinear, and soft matter physics* **2008**, *77* (5), 051202.

(55) Klein, R. J.; Zhang, S.; Dou, S.; Jones, B. H.; Colby, R. H.; Runt, J. Modeling electrode polarization in dielectric spectroscopy: Ion mobility and mobile ion concentration of single-ion polymer electrolytes. *J. Chem. Phys.* **2006**, *124* (14), 144903.

(56) Kirchner, B. *Ionic Liquids*, 1st ed.; Springer-Verlag: Berlin, 2010; p 346.

(57) Wang, S.-W.; Liu, W.; Colby, R. H. Counterion Dynamics in Polyurethane-Carboxylate Ionomers with Ionic Liquid Counterions. *Chem. Mater.* **2011**, *23* (7), 1862−1873.

(58) Dyre, J. C.; Hechsher, T.; Niss, K. A brief critique of the Adam−Gibbs entropy model. *J. Non-Cryst. Solids* **2009**, *355* (10−12), 624−627.

(59) Wojnarowska, Z.; Paluch, K. J.; Shoifet, E.; Schick, C.; Tajber, L.; Knapik, J.; Wlodarczyk, P.; Grzybowska, K.; Hensel-Bielowka, S.; Verevkin, S. P.; Paluch, M. Molecular origin of enhanced proton conductivity in anhydrous ionic systems. *J. Am. Chem. Soc.* **2015**, *137* (3), 1157−64.

(60) Wojnarowska, Z.; Knapik, J.; Jacquemin, J.; Berdzinski, S.; Strehmel, V.; Sangoro, J. R.; Paluch, M. Effect of Pressure on Decoupling of Ionic Conductivity from Segmental Dynamics in Polymerized Ionic Liquids. *Macromolecules* **2015**, *48* (23), 8660−8666.

(61) Wojnarowska, Z.; Knapik, J.; Díaz, M.; Ortiz, A.; Ortiz, I.; Paluch, M. Conductivity Mechanism in Polymerized Imidazolium-Based Protic Ionic Liquid [HSO3−BVIm][OTf]: Dielectric Relaxation Studies. *Macromolecules* **2014**, *47* (12), 4056−4065.

(62) Wojnarowska, Z.; Roland, C. M.; Swiety-Pospiech, A.; Grzybowska, K.; Paluch, M. Anomalous Electrical Conductivity Behavior at Elevated Pressure in the Protic Ionic Liquid Procainamide Hydrochloride. *Phys. Rev. Lett.* **2012**, *108* (1), 015701.

(63) Franke, M. E.; Simon, U. Proton mobility in H-ZSM5 studied by impedance spectroscopy. *Solid State Ionics* **1999**, *118* (3−4), 311−316.

(64) la Cruz, D. S.-d.; Green, M. D.; Ye, Y.; Elabd, Y. A.; Long, T. E.; Winey, K. I. Correlating backbone-to-backbone distance to ionic conductivity in amorphous polymerized ionic liquids. *J. Polym. Sci., Part B: Polym. Phys.* **2012**, *50* (5), 338−346.

(65) Bruce, P. G. *Solid State Electrochemistry*; Cambridge University Press: Cambridge, UK, 1995.

(66) Lovell, R.; Windle, A. H. Determination of the local conformation of PMMA from wide-angle X-ray scattering. *Polymer* **1981**, *22* (2), 175−184.

(67) Arbe, A.; Genix, A. C.; Colmenero, J.; Richter, D.; Fouquet, P. Anomalous relaxation of self-assembled alkyl nanodomains in high-order poly(n-alkyl methacrylates). *Soft Matter* **2008**, *4* (9), 1792−1795.

(68) Green, M. D.; Salas-de la Cruz, D.; Ye, Y.; Layman, J. M.; Elabd, Y. A.; Winey, K. I.; Long, T. E. Alkyl-Substituted N-Vinylimidazolium Polymerized Ionic Liquids: Thermal Properties and Ionic Conductivities. *Macromol. Chem. Phys.* **2011**, *212* (23), 2522−2528.

DOI: 10.1021/acs.macromol.8b01273